




Pseudomonas aeruginosa survives in epithelia by ExoS-mediated inhibition of autophagy and mTOR

Lang Rao^{1,2,3,*†} , Indhira De La Rosa^{1,†}, Yi Xu¹, Youbao Sha¹, Abhisek Bhattacharya¹ ,
Michael J Holtzman⁴, Brian E Gilbert⁵ & N Tony Eissa^{1,2} 

Abstract

One major factor that contributes to the virulence of *Pseudomonas aeruginosa* is its ability to reside and replicate unchallenged inside airway epithelial cells. The mechanism by which *P. aeruginosa* escapes destruction by intracellular host defense mechanisms, such as autophagy, is not known. Here, we show that the type III secretion system effector protein ExoS facilitates *P. aeruginosa* survival in airway epithelial cells by inhibiting autophagy in host cells. Autophagy inhibition is independent of mTOR activity, as the latter is also inhibited by ExoS, albeit by a different mechanism. Deficiency of the critical autophagy gene *Atg7* in airway epithelial cells, both *in vitro* and in mouse models, greatly enhances the survival of ExoS-deficient *P. aeruginosa* but does not affect the survival of ExoS-containing bacteria. The inhibitory effect of ExoS on autophagy and mTOR depends on the activity of its ADP-ribosyltransferase domain. Inhibition of mTOR is caused by ExoS-mediated ADP ribosylation of RAS, whereas autophagy inhibition is due to the suppression of autophagic Vps34 kinase activity.

Keywords ADP-ribosyltransferase; autophagy; ExoS; mTOR;
Pseudomonas aeruginosa

Subject Categories Microbiology, Virology & Host Pathogen Interaction;
Post-translational Modifications & Proteolysis; Signal Transduction

DOI 10.15252/embr.202050613 | Received 9 April 2020 | Revised 29 October 2020 | Accepted 12 November 2020 | Published online 20 December 2020

EMBO Reports (2020) 22: e50613

Introduction

The luminal surface of the respiratory tract is covered with airway epithelial cells, including ciliated, basal, and Clara cells, which share the common goal of maintaining an antimicrobial environment in the respiratory tract (Crystal *et al.*, 2008). Airway epithelial cells employ various methods to prevent pathogen colonization (Diamond *et al.*, 2000; Li *et al.*, 2012). They act as a cellular barrier,

generate antimicrobial agents, and recruit neutrophils and macrophages to the site of infection. In addition, studies have suggested that airway epithelial cells are able to promote the clearance of internalized bacteria (Cortes *et al.*, 2002). A damaged airway epithelial barrier or a weakened immune system allows opportunistic pathogens to invade and persist in airway epithelial cells (Williams *et al.*, 2010).

Pseudomonas aeruginosa bacterium is an opportunistic pathogen that typically targets the respiratory tract in patients who are immunocompromised and is frequently responsible for hospital-acquired pneumonia (Yasmin *et al.*, 2006). In these conditions, severe pneumonia and bronchitis can develop with a high rate of mortality (Scheetz *et al.*, 2009). Chronic *P. aeruginosa* infection occurs in subjects with cystic fibrosis (Goldberg & Pier, 2000; Scheetz *et al.*, 2009). *Pseudomonas aeruginosa* has evolved methods to successfully colonize and damage airway epithelium (Hauser, 2009). The type III secretion system (T3SS) is a virulence mechanism that allows *P. aeruginosa* to inject up to four cytotoxins ExoS, ExoT, ExoU, and ExoY into host cells (Vance *et al.*, 2005). ExoS and ExoT are bifunctional enzymes that contain an N-terminal small GTPase-activating protein (GAP) domain and C-terminal ADP-ribosyltransferase (ADPRT) domain (Barbieri & Sun, 2004). The GAP domains in ExoS and ExoT inhibit Rho-like GTPases, including Rho, Rac1, and CDC42 (Kazmierczak *et al.*, 2004). The ADPRT domain of ExoT targets CrkI and CrkII, whereas that of ExoS negatively regulates several host cell substrates including Ras-like GTPases (Ganesan *et al.*, 1998; Ganesan *et al.*, 1999b). Importantly, ExoS is critical for the survival of *P. aeruginosa* in epithelial cells, though the underlying mechanisms remain unidentified (Angus *et al.*, 2010).

Autophagy is characterized by the formation of double-membrane organelles called autophagosomes, which engulf cytoplasmic components and induce their degradation after fusion with lysosomes. Autophagy is a key process in innate immunity and pathogen clearance, and pathogens have evolved ways to evade autophagy (Levine & Deretic, 2007; Rao & Eissa, 2020). During lung infection by *P. aeruginosa*, autophagy plays an important role in mast cells and alveolar macrophages in the clearance of the bacteria

1 Department of Medicine, Baylor College of Medicine, Houston, TX, USA

2 Veterans Administration Long Beach Health Care System and University of California at Irvine, Irvine, CA, USA

3 Southern California Institute for Research and Education, Long Beach, CA, USA

4 Department of Internal Medicine, Washington University School of Medicine, St. Louis, MO, USA

5 Department of Molecular Virology and Microbiology, Baylor College of Medicine, Houston, TX, USA

*Corresponding author. Tel: +01 562 826 8000; X-15676; E-mail: Lang.Rao@va.gov

†These authors contributed equally to this work

(Yuan *et al.*, 2012). However, the role of autophagy in innate immune functions of airway epithelium is not well studied. Further, the relationship between autophagy and *P. aeruginosa* in airway epithelial cells has not been elucidated. Specifically, it is not known if *P. aeruginosa* could modulate autophagy to facilitate its survival in airway epithelial cells. Previous studies showed that *P. aeruginosa* could survive and multiply in airway epithelial cells without any evidence of elimination by the lysosomes (Chi *et al.*, 1991). In corneal epithelial cells, the mutant *P. aeruginosa* lacking the T3SS showed more colocalization with the lysosomal markers compared to the WT *P. aeruginosa* (Angus *et al.*, 2010). In addition, an *in vivo* study indicated that T3SS mutant *P. aeruginosa* is more susceptible to elimination by host cells than its wild type counterpart (Vance *et al.*, 2005). These studies suggest that the T3SS of *P. aeruginosa* might play a role in overcoming the host defense mechanisms to facilitate its survival in epithelial cells. In addition to the need to evade host defense, pathogens can benefit from inhibiting host protein synthesis. However, inhibition of the mTOR pathway, as a pathogen strategy to inhibit host protein synthesis, could endanger pathogen survival because mTOR inhibition would activate autophagy (Kim *et al.*, 2011). Here, we show that *P. aeruginosa* simultaneously inhibits both the mTOR pathway and autophagy through independent mechanisms. Remarkably, the T3SS effector protein ExoS mediates both the inhibitory mechanisms through its ExoS ADPRT activity. These mechanisms are critical for the survival of *P. aeruginosa* in airway epithelial cells *in vitro* and *in vivo*.

Results

***Pseudomonas aeruginosa* T3SS protected *Pseudomonas aeruginosa* from autophagy elimination**

Pathogens are commonly targeted to the autophagy-lysosomal pathway by host cells as a strategy to contain their replication and limit the infection (Nakagawa *et al.*, 2004). In order to persist inside host cells, pathogens have evolved strategies to evade or inhibit autophagy (Ogawa *et al.*, 2005; Jia *et al.*, 2009). Existing evidence suggests that *P. aeruginosa* T3SS is required for their intracellular survival (Angus *et al.*, 2010) but the underlying mechanisms are not known. We hypothesized that *P. aeruginosa* T3SS promoted the survival of *P. aeruginosa* in airway epithelial cells by suppressing autophagy. To test this hypothesis, we generated a cell line of type II alveolar human epithelial cells line A549 that stably expressed shRNA against autophagy-related gene 7 (*Atg7*) we termed A549-(*Atg7*⁻) and a control cell line expressing non-target shRNA, termed A549-(*Atg7*⁺). We confirmed the reduction of autophagy in A549-(*Atg7*⁻) cells by immunoblotting. Compared to the control cells, A549-(*Atg7*⁻) cells showed an accumulation of autophagy substrate SQSTM1 (also known as p62), and a reduction of *Atg7* and LC3 type II (Fig 1A). To investigate if autophagy in airway epithelial cells was required to control bacterial pathogens, we first tested the effect of autophagy deficiency on the intracellular survival of airway epithelium pathogen *Klebsiella pneumoniae* (Cortes *et al.*, 2002). We infected both A549-(*Atg7*⁻) and A549-(*Atg7*⁺) cells with *K. pneumoniae* for 1 and 4 h, followed by 1 h of gentamycin treatment to kill extracellular bacteria. We then evaluated the intracellular bacterial load using colony-forming units (CFU) assay. After 4 h of infection, a

significantly higher number of bacteria was recovered from the autophagy-deficient A549-(*Atg7*⁻) cells, compared to their control counterpart (Fig 1B). This result showed that autophagy was important for *K. pneumoniae* elimination in airway epithelial cells. We then conducted similar experiments utilizing wild-type *P. aeruginosa* or *ΔpscD P. aeruginosa*, a mutant strain that contains the three cytotoxins but is deficient in the T3SS translocation apparatus (Stover *et al.*, 2000; Miao *et al.*, 2008; Sun *et al.*, 2012; Fig 1C). There was no significant difference between the CFU counts of WT *P. aeruginosa* recovered from A549-(*Atg7*⁺) and A549-(*Atg7*⁻) cells 4 h post-infection (Fig 1D). In contrast, CFU counts of the mutant *ΔpscD P. aeruginosa* were markedly reduced in A549-(*Atg7*⁺) cells compared to autophagy-deficient A549-(*Atg7*⁻) cells (Fig 1E). In both bacterial infections, there was no substantial difference in recovered CFU after 1-h infection period, indicating that autophagy deficiency, rather than an internalization defect, was responsible for the reduction in bacterial survival. Taken together, these data showed that WT, but not T3SS-deficient mutant *P. aeruginosa*, could resist elimination by autophagy.

We then speculated that autophagy inhibition by WT *P. aeruginosa* allowed the bacteria to survive in A549 cells. To determine the effect of *P. aeruginosa* on autophagy, we infected A549 cells with WT *P. aeruginosa* for various time points and evaluated the generation of the autophagy marker LC3 type II (LC3II) by immunoblotting of cell lysates (Fig 2A). The T3SS of *P. aeruginosa* PAO1 strain secretes the effector proteins ExoS, ExoT, and ExoY. Using specific antibodies, we were able to detect the presence of the effector toxins in cell lysates of A549 cells as early as 2 h post-infection (Fig 2A). More importantly, concomitant with the expression of T3SS effector proteins following infection, there was a corresponding reduction in autophagy marker LC3II (Fig 2A). Given autophagy marker protein LC3II are affected by LC3I to LC3II conversion, as well as lysosomal mediated degradation. We infected A549 cells with either *P. aeruginosa* WT or *ΔpscD* mutant under the treatment of lysosomal inhibitor chloroquine (CQ) (Klionsky *et al.*, 2008). Levels of autophagy marker LC3II were decreased in cells infected with WT *P. aeruginosa* compared with cells infected with *ΔpscD* mutant or with non-infected cells (Fig 2B). This finding suggested that LC3II reduction found in WT *P. aeruginosa*-infected cells was caused by the decreased generation of LC3II, rather than by increased lysosomal degradation of LC3II. *P. aeruginosa*' T3SS is known to induce cell death in the host cells (Jia *et al.*, 2006). We thus determined cell death and find that although cell death was higher in cells infected with T3SS-competent *P. aeruginosa* compared to those infected T3SS-deficient *P. aeruginosa*, the overall cell death rate was less than 10% in both conditions (Fig EV1A and B). These data suggested that the significant reduction of LC3II caused by WT *P. aeruginosa* was not simply caused by increased cell death.

To further evaluate the effect of *P. aeruginosa*' T3SS on autophagy, we generated A549 cell line stably expressing the autophagy marker LC3 fused to green fluorescent protein (GFP-LC3). In these cells, the formation of autophagosomes is accompanied by changes in the distribution of GFP-LC3 from diffuse cytosolic staining to punctate fluorescence bodies (Levine & Deretic, 2007). We then infected these cells with WT or *ΔpscD P. aeruginosa*. There was increased GFP-LC3 autophagosomes only in cells infected with the *ΔpscD P. aeruginosa* mutant strain, compared to non-infected cells

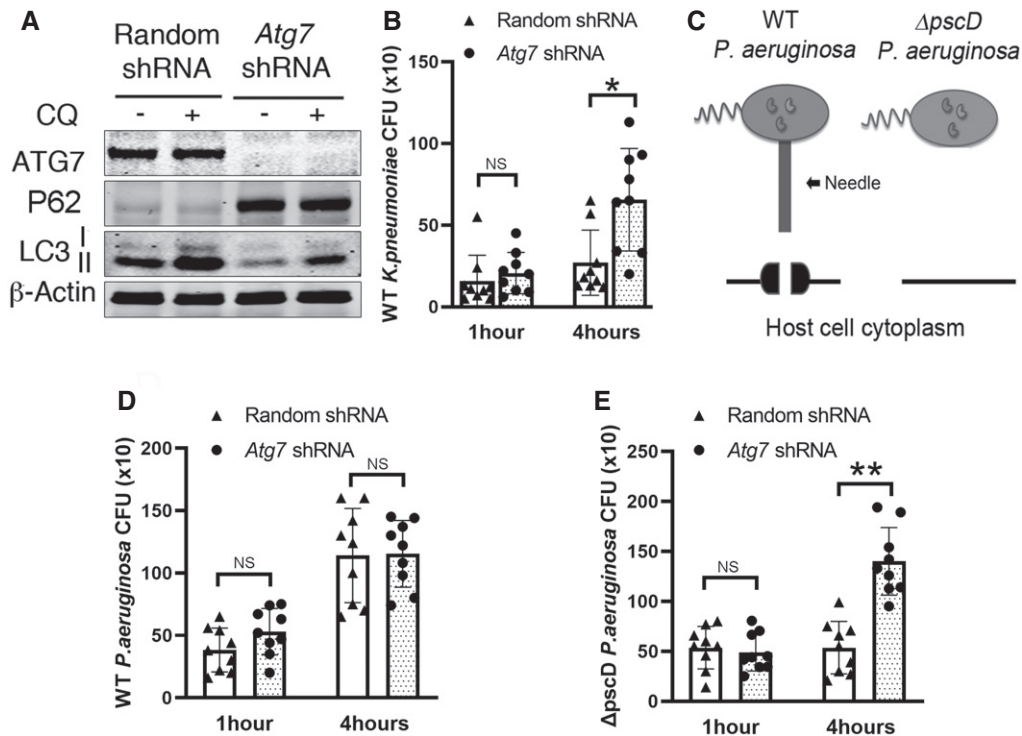


Figure 1. *Pseudomonas aeruginosa* T3SS protected *P. aeruginosa* from autophagy elimination.

A549 cells stably expressing lentivirus vector containing random shRNA or *Atg7* specific shRNA were generated.

A Cells were incubated for 2 h in the presence or absence of 50 nM of lysosomal inhibitor chloroquine (CQ). Cell lysates were evaluated by immunoblotting.

B Cells were infected, for 1 and 4 h, with *K. pneumoniae* at MOI of 10 followed by 1 h of gentamycin treatment. Cell lysates were plated in LB agar for 18 h and CFU were determined.

C Schematic of WT *P. aeruginosa* and *ΔpscD P. aeruginosa* mutant.

D, E Cells were infected, for 1–4 h, with WT (D) or *ΔpscD P. aeruginosa* (E) at MOI of 10. All infections were followed by 1 h of gentamycin treatment. Cell lysates were plated in LB agar for 18 h and CFU were determined.

Data information: In (B) and (D, E), the triangles and dots represent the individual test (three technical replicates per individual test) on control and *Atg7* knock down cells. The bars represent the mean CFU of each group (three biological replicates each group), error bars represent standard deviation. Statistical significance between assays was calculated using two-tailed Student's *t*-test with Welch's correction. NS: not significant; * $P \leq 0.05$; ** $P \leq 0.01$.

Source data are available online for this figure.

or to cells infected with WT *P. aeruginosa* (Fig 2C). These data confirmed that autophagy was attenuated by WT *P. aeruginosa* T3SS.

We then decided to investigate whether or not the induction of autophagy by rapamycin (an mTOR inhibitor) could overcome the inhibitory effect of *P. aeruginosa* T3SS. We treated A549 cells with DMSO or rapamycin before bacterial infection. We found no difference in the survival of WT *P. aeruginosa* in cells treated with rapamycin compared to cells treated with vehicle (Fig 2D). In contrast, in A549 cells infected with *ΔpscD P. aeruginosa*, there was a marked reduction in the viability of bacteria in A549 cells treated with rapamycin (Fig 2E). The immunoblotting assay showed rapamycin inhibited mTOR and induced autophagy, as evidenced by the reduction of mTOR downstream target phospho-S6 and increased LC3II respectively (Fig EV2A). Interestingly, A549 cells treated with rapamycin and infected with WT *P. aeruginosa* still showed a reduced LC3II when compared to non-infected cells (Fig EV2A). Similar results were found following exogenous overexpression of the ExoS-encoding construct in A549 cells (Fig EV2B). These findings suggested that rapamycin could not restore autophagy inhibition caused by T3SS. Taken together, these results indicated that

T3SS facilitates the intracellular survival of WT *P. aeruginosa* by inhibiting autophagy. They further implied that *P. aeruginosa* inhibited autophagy by a mechanism independent of mTOR signaling pathway.

The *Pseudomonas aeruginosa* ExoS was required and sufficient for autophagy inhibition

The *P. aeruginosa* T3SS is composed of several proteins including translocation proteins, chaperones and effectors proteins (Hauser, 2009). It has been shown that *P. aeruginosa* T3SS effector proteins contribute the most to *P. aeruginosa* pathogenesis (Williams *et al*, 2010). They are also found to negatively modulate different intracellular pathways (Hauser, 2009). Therefore, we hypothesized that *P. aeruginosa* T3SS effector proteins were responsible for autophagy inhibition. To determine which effectors proteins were implicated in such effect, we chose different *P. aeruginosa* mutants (deficient in one or more of the three T3SS effectors proteins ExoS, ExoT, and ExoY) to infect A549 cell line and primary human bronchial epithelial cells (NHBE). By evaluating formation of LC3II (Fig 3A and B)

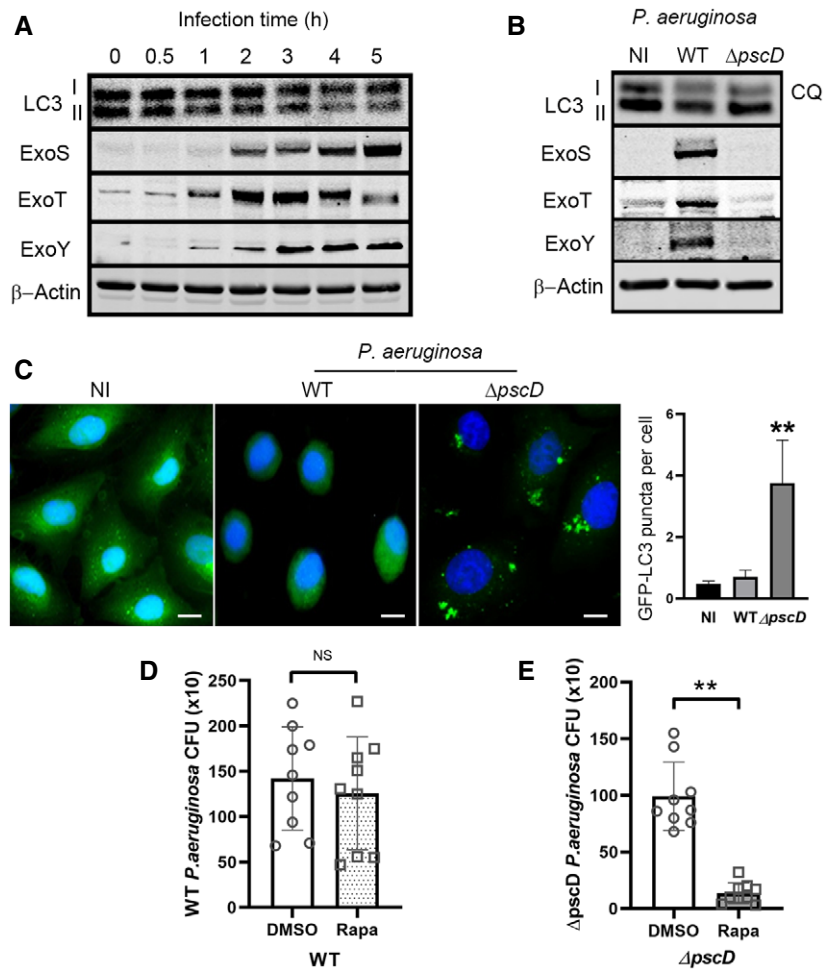


Figure 2. *Pseudomonas aeruginosa* inhibited autophagy by a T3SS-dependent mechanism.

- A A549 cells were infected with WT *P. aeruginosa* for various time points and cell lysates were evaluated by immunoblotting.
- B A549 cells infected with WT or Δ pscD *P. aeruginosa* for 4 h or left uninfected (NI) in the presence of lysosomal inhibitor CQ (50 nM). The cell lysates were evaluated by immunoblotting.
- C A549 cells stably expressing GFP-LC3 were left non-infected or infected, for 4 h, with WT or Δ pscD *P. aeruginosa*, and evaluated by fluorescence microscopy. Cell nuclei were counterstained with DAPI (blue) and autophagosome were visualized as green puncta. Graph represents quantitative analysis of GFP-LC3-positive autophagosome per cell, scale bars: 10 μ m. Each bar represents mean value of three independent experiments, error bars represent standard deviation. Statistical significance between assays was determined using One-way ANOVA followed by Dunn's Multiple-comparison test. ** $P \leq 0.01$.
- D, E A549 cells were treated for 16 h with rapamycin 0.8 μ g/ml or DMSO, then infected with either WT (D) or Δ pscD *P. aeruginosa* and followed by 1 h of gentamycin treatment (E). The circles and squares represent the individual test (three technical replicates per individual test) with DMSO and rapamycin treatment. The bars represent the means of CFU from three independent experiments, error bars represent standard deviation. The significance of differences between different drug treatment was determined using two-tailed Student's *t*-test with Welch's correction. NS: not significant; * $P \leq 0.05$; ** $P \leq 0.01$.

Source data are available online for this figure.

and GFP-LC3 puncta (Fig 3C), we found cells infected with bacteria containing ExoS *P. aeruginosa* (WT, Δ TY) had reduced autophagy compared to cells infected with bacteria not containing ExoS *P. aeruginosa* (Δ S and Δ TY) (Fig 3A–C). Importantly, ExoS was the only toxin, among those tested, that was required for the inhibition of autophagy. Bacteria containing only ExoT (Δ SY) or ExoY (Δ ST) but lacking ExoS did not reduce LC3II formation (Fig EV3A). Limited cell death (< 15% of whole cell population) (Fig EV1C and D) was detected in these experiments suggesting that the marked reduction in LC3II and GFP-LC3 puncta could not be simply the result of cell death caused by ExoS-containing *P. aeruginosa*.

We also examined ExoS's effect on autophagic flux in cells expressing a tandem fluorescent RFP-GFP-tagged LC3. As GFP fluorescence signal gets quenched in acidic environment inside lysosome lumen, autophagosomes are visualized as yellow puncta (the overlay of green and red fluorescence), while autolysosomes are visualized as red puncta only (Klionsky *et al*, 2008). We found cells infected with ExoS-containing *P. aeruginosa* exhibited a marked reduction in both autophagosomes (yellow puncta) and autolysosomes (red puncta) (Fig EV4). It suggested ExoS affects autophagy by inhibiting autophagosome formation, instead of increasing autophagosome–lysosome fusion.

ExoS protected *Pseudomonas aeruginosa* from elimination by host autophagy

Previous studies suggested ExoS is required for *P. aeruginosa* survival within epithelial cells (Angus *et al*, 2010). We reasoned that ExoS promoted intracellular *P. aeruginosa* viability by inhibiting autophagy. We infected A549 cells, stably expressing GFP-LC3, with WT, ΔS , ΔTY , and ΔSTY *P. aeruginosa* and analyzed their colocalization with GFP-LC3 autophagosomes. We found in infected cells, ExoS-deficient *P. aeruginosa* (ΔS and ΔSTY) colocalized

significantly more than ExoS-containing *P. aeruginosa* (WT and ΔTY) with GFP-LC3 autophagosomes (Fig 3D and E). Further, in cells infected with ExoS-expressing *P. aeruginosa* (WT and ΔTY), the GFP-LC3 remained mostly diffused indicating that they did not form autophagosomes (Fig 3D and E). This finding suggested that ExoS might protect *P. aeruginosa* from being engulfed into autophagosome. We also confirmed the result by electron microscopy assays. We found ΔSTY *P. aeruginosa* were engulfed by multiple membrane autophagosome, whereas ΔTY *P. aeruginosa* were found in cytoplasm (Fig 3F).

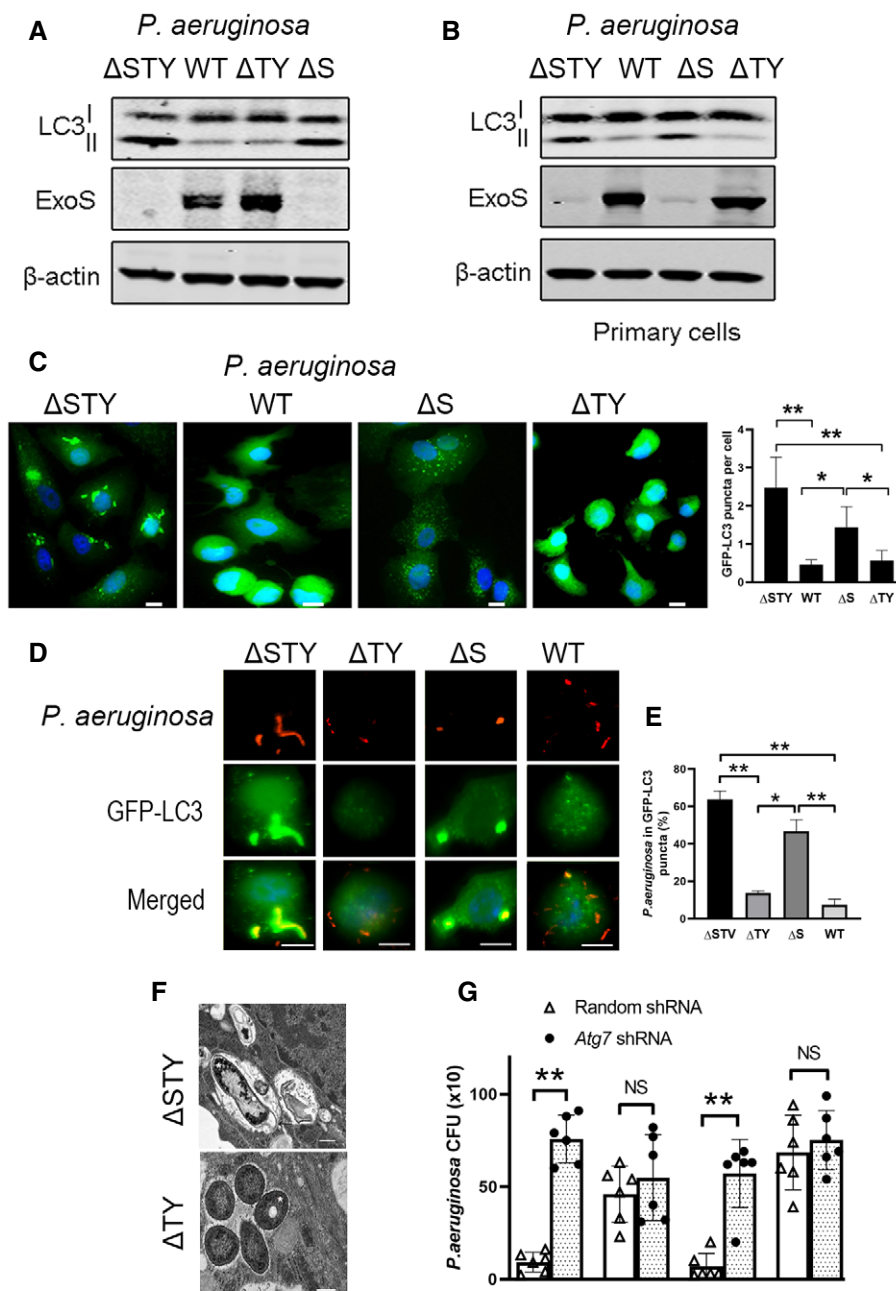


Figure 3.

Figure 3. The *Pseudomonas aeruginosa* ExoS was required and sufficient for autophagy inhibition. ExoS protected *P. aeruginosa* from autophagy elimination.

- A, B (A) A549 cells or (B) primary human bronchial epithelial cells were infected with one of several *P. aeruginosa* mutants. Cell lysates were evaluated by immunoblotting.
- C A549 cells, stably expressing GFP-LC3, were infected with WT or *P. aeruginosa* mutants and evaluated by fluorescence microscopy, scale bars: 10 μm . GFP-LC3 puncta representing the autophagosomes was quantified and presented in the graph. Each bar represents mean value from three independent experiments and error bars represent standard deviation. Statistical significance between assays was determined using one-way ANOVA followed by Dunn's multiple-comparison test. * $P \leq 0.05$; ** $P \leq 0.01$. *P. aeruginosa* mutant strains legend: ΔSTY (mutant deficient for the three cytotoxins), WT (contains all cytotoxin), ΔS (deficient for ExoS but still express ExoT and ExoY), ΔTY (express ExoS but deficient for ExoT and ExoY).
- D, E A549 cells, stably expressing GFP-LC3, were infected for 4 h with WT or with one of *P. aeruginosa* mutants (ΔSTY , ΔS and ΔTY) and evaluated by fluorescence microscopy (D). *Pseudomonas aeruginosa* were visualized using specific antibody (red) and the colocalized bacteria signals with GFP-LC3 puncta (green) were merged and presented as yellow. Scale bars: 10 μm . (E) Quantitative analysis of colocalization of internalized *P. aeruginosa* with GFP-LC3-positive puncta. The colocalization of these two signals was quantified with 10 independent visual fields of more than 100 cells. Data represent mean \pm SD of three independent experiments. Statistical significance between assays was determined using One-way ANOVA followed by Dunn's multiple-comparison test. * $P \leq 0.05$; ** $P \leq 0.01$.
- F Representative transmission electron microscopy images of A549 cells infected with *P. aeruginosa* containing ExoS (ΔTY) or deficient for the three T3SS effector proteins (ΔSTY) for 4 h. ΔSTY *P. aeruginosa* (white star) was engulfed by multiple membrane autophagosomes (black arrow). ΔTY *P. aeruginosa* (white star) were found in cytoplasm with single membrane surrounded, scale bars: 0.5 μm .
- G A549 cells, stably expressing lentiviral vectors containing random shRNA or Atg7 shRNA, were infected with WT or *P. aeruginosa* mutants (ΔSTY , ΔTY , and ΔS) at MOI of 10. All infections were followed by 1 h of gentamycin treatment. Cell lysates were plated in LB agar for 18 h, and CFU were determined. The triangles and dots represent the individual test (three technical replicates per individual test) on control and Atg7 knock down cells from three biological replicates. The bars represent the means of CFU of each group (three biological replicates each group), error bars represent standard deviation. The significance of differences between different assay was determined using two-tailed Student's *t*-test with Welch's correction, NS: not significant; ** $P \leq 0.01$.

Source data are available online for this figure.

We then evaluated the ability of autophagy to eliminate intracellular *P. aeruginosa* by determining bacterial survival following infection of normal A549-(Atg7⁺) or autophagy-deficient cell line A549-(Atg7⁻). ExoS-expressing *P. aeruginosa* (WT or ΔTY) survived to a similar extent in both A549-(Atg7⁺) and A549-(Atg7⁻) cells. In contrast, ExoS-deficient *P. aeruginosa* (ΔS or ΔSTY) viability was markedly reduced in A549-(Atg7⁺) cells, compared to A549-(Atg7⁻) (Fig 3G). These data suggested that reduction of autophagy in A549 cells enhanced the survival of ExoS-deficient *P. aeruginosa*. Taken together, these results showed that ExoS is the main T3SS effector that protected *P. aeruginosa* from autophagy-mediated elimination.

ExoS protected *Pseudomonas aeruginosa* from autophagy-mediated elimination *in vivo*

The above *in vitro* study on epithelial cells indicated ExoS facilitates bacterial survival by inhibiting autophagy. We wonder if ExoS had a similar effect *in vivo*. We generated conditional knockout Atg7 Δ mice with Atg7 deficient in ciliated airway epithelial cells by breeding FOXJ1-Cre mice with Atg7 flox/flox mice. In transgenic Atg7 Δ mice, Atg7 depletion in mouse tracheal airway epithelial cells was validated by immunoblotting and immunofluorescence microscopy (Fig 4A and B). Further, accumulation of P62 and diminished LC3II confirmed autophagy deficiency in these cells (Fig 4A). Examination of lung, spleen and liver from Atg7 Δ mice revealed no gross abnormalities and Atg7 Δ mice had similar life span to wild-type Atg7 flox/flox mice. We infected both Atg7 Δ and Atg7 flox/flox mice with a non-lethal dose (3×10^7 CFU) of wild-type or *P. aeruginosa* mutants. 24 h post-infection, bacterial CFU in the lungs were quantitated. No significant difference in bacterial CFU was observed in mice infected with ExoS-expressing *P. aeruginosa* (WT or ΔTY). In contrast, a higher bacterial count was observed in autophagy-deficient Atg7 Δ mice when infected with ExoS-deficient (ΔS or ΔSTY) *P. aeruginosa* than in normal mice (Atg7 flox/flox) (Fig 4C). These results suggested that, *in vivo*, ExoS protects *P. aeruginosa* from elimination by autophagy. We also

dissected bacterial dissemination in spleen and liver. Similar to the lungs, no difference in bacterial counts was found in liver and spleen from *P. aeruginosa* (ΔTY) infected mice. From *P. aeruginosa* (ΔSTY) infected mice, we also found higher bacterial counts in Atg7 Δ mice compared to Atg7 flox/flox mice (Fig 4D). Moreover, higher *P. aeruginosa* (ΔTY) counts than *P. aeruginosa* (ΔSTY) was found in all these organs (Fig 4D) which is likely due to ExoS's ability in facilitating *P. aeruginosa* dissemination by breaking pulmonary vascular barrier (Rangel et al, 2015).

We evaluated survival of Atg7flox/flox and Atg7 Δ mice in response to lethal dose (1×10^9 CFU) of *P. aeruginosa* infection. With *P. aeruginosa* (ΔTY) infection, there was no significant difference in survival rate between the two groups of mice (Fig 4E). In contrast, when infected with (ΔSTY) *P. aeruginosa*, survival rate was significantly reduced in Atg7 Δ mice compared to wild-type mice (Fig 4F). We believe the higher mortality resulted from higher bacterial burden inside of these autophagy-deficient mice. Together, these experiments suggest that the *P. aeruginosa* effector protein ExoS protects the bacteria from elimination by autophagy *in vivo*. In addition, it also points out the importance of autophagy in airway epithelial cells for the clearance of *P. aeruginosa*.

ADP-ribosyl transferase activity of ExoS was required for autophagy inhibition by *Pseudomonas aeruginosa*

ExoS is a bifunctional enzyme that contains both GTPase-activating protein and ADP-ribosyltransferase ADPRT domain (Barbieri & Sun, 2004). We wanted to determine which domain was responsible for autophagy inhibition. We infected cells with wild-type *P. aeruginosa* or strains containing point mutations in the GAP or ADPRT domains of ExoS. We found that *P. aeruginosa* strains with intact ExoS ADPRT activity, that is, WT or *P. aeruginosa* with ExoS-containing ADPRT activity but mutated for the GAP activity (S^{G-A+}), were able to inhibit autophagy and reduce LC3II generation in both A549 and NHBE cells (Figs 5A and EV3B). In contrast, *P. aeruginosa* strains containing ExoS lacking ADPRT activity, that is, *P. aeruginosa* with

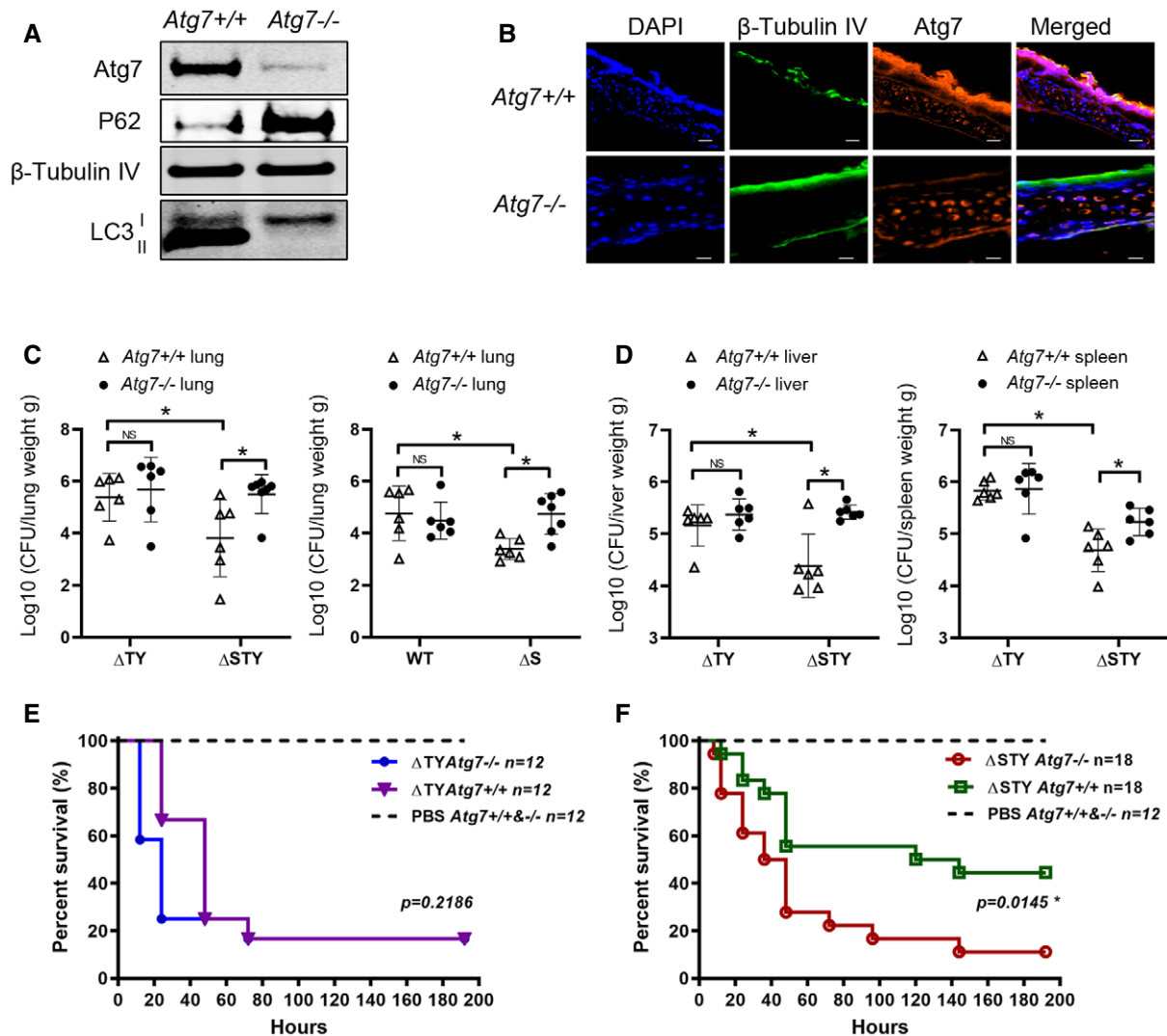


Figure 4. ExoS protected *Pseudomonas aeruginosa* from autophagy elimination *in vivo*.

- A Primary airway epithelial cells were isolated from tracheas of *Atg7^{+/+}* and *Atg7^{-/-}* mouse and were evaluated by immunoblotting.
- B Sections of tracheas from *Atg7^{+/+}* and *Atg7^{-/-}* mouse were evaluated by immunofluorescence microscopy following staining of nuclear DNA with DAPI (Blue), ciliated epithelial cell marker β -tubulin IV (green) and Atg7 (red). Scale bars: 20 μ m.
- C, D *Atg7^{+/+}* and *Atg7^{-/-}* mice were intranasally injected with 3×10^7 CFU of WT, Δ S, Δ TY or Δ STY *P. aeruginosa*. After 24 h, lungs (C), spleens and livers (D) were harvested, homogenized and diluted for CFU counting. Each data point represents bacterial count (Log_{10} CFU/g) from individual mouse. The horizontal lines represent the mean value from each group (6 mice each group), error bars represent standard deviation. The significance of differences between different drug treatment was determined using one-way ANOVA and Dunn's multiple-comparison test, NS: not significant; * $P \leq 0.05$
- E, F *Atg7^{+/+}* and *Atg7^{-/-}* mice were intranasally injected with PBS with or without 1×10^9 CFU of Δ TY (E) Δ STY (F). Mice survival was monitored for 10 days post-infection. Kaplan-Meier survival curves were made based on the observation of 12–18 mice/group from two independent experiments. The P -values were calculated using the log-rank test (Δ TY $\text{Atg7}^{+/+}$ vs. Δ TY $\text{Atg7}^{-/-}$, $P = 0.2186$; Δ STY $\text{Atg7}^{+/+}$ vs. Δ STY $\text{Atg7}^{-/-}$, $P = 0.0145$).

Source data are available online for this figure.

ExoS mutated in ADRPT domain (S^{G+A-}) or with ExoS lacking both GAP and ADPRT activity (S^{G-A-}) were not able to inhibit autophagy (Figs 5A and EV3B). These data suggested that ADPRT activity of ExoS was required for *P. aeruginosa* inhibitory effect on autophagy.

We then wanted to determine if ADPRT activity of ExoS was sufficient to inhibit autophagy in the absence of any other bacterial products. We transfected A549 cells with plasmids expressing ExoS (WT), ExoS without ADPRT activity (S^{G+A-}) or ExoS with no GAP or ADPRT activity (S^{G-A-}). Transfection of cells with plasmids

containing WT ExoS resulted in inhibition of autophagy, as evidenced by reduction of LC3II formation, whereas plasmids containing mutated ExoS lacking ADPRT activity had no such effect (Fig 5B). In additional experiments, A549 cells were pre-treated with the ADPRT inhibitor *m*-iodobenzylguanidine hemisulfate salt (MIBG), which competes with the arginine residues of target proteins for the ADP-ribose group, thereby inhibiting the ADPRT effect on target molecules (Loesberg *et al*, 1990). Pre-treatment of cells with MIBG prevented the reduction of autophagy marker LC3II

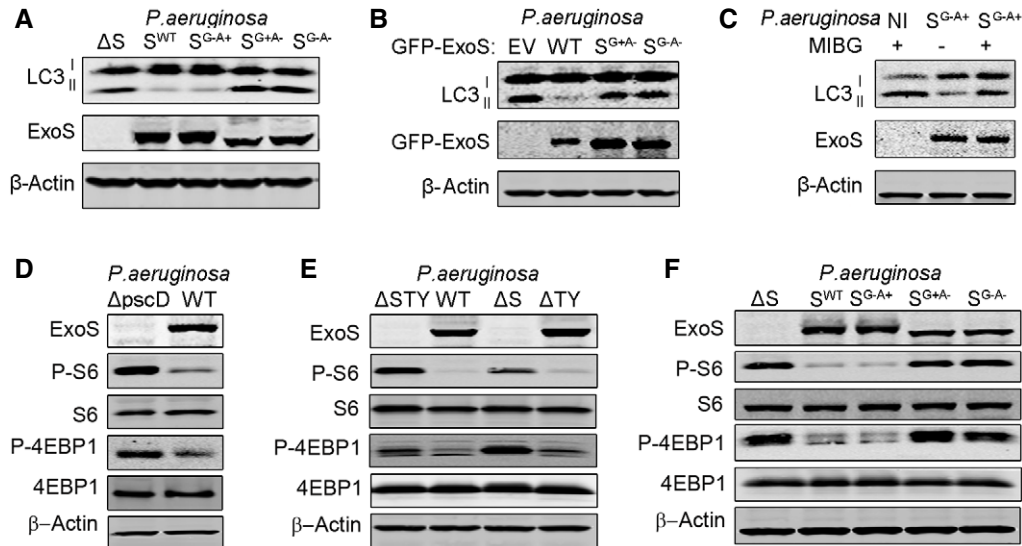


Figure 5. ExoS ADP-ribosyltransferase activity inhibited autophagy and mTOR signaling pathway.

A, F A549 cells were infected for 4 h with ExoS-deficient *P. aeruginosa* (ΔS), ExoS-containing *P. aeruginosa* (S^{WT}), *P. aeruginosa* containing ExoS with loss-of-function mutations in the GTPase-activating domain (S^{G-A+}), in the ADP ribosylation domain (S^{G+A-}), or in both domains (S^{G-A-}). Cell lysates were evaluated by immunoblotting.

B A549 cells were transfected, for 24 h, with a plasmid expressing empty vector (EV), WT GFP-ExoS, a GFP-ExoS mutant for ADPRT domain (S^{G+A-}) or a GFP-ExoS mutant deficient in both GAP and ADPRT domains (S^{G-A-}). Cell lysates were evaluated by immunoblotting.

C A549 cells were treated for 24 h with 100 μ M of the ADPRT activity inhibitor MIBG and then left uninfected (NI) or infected with *P. aeruginosa* containing ExoS with ADPRT activity only (S^{G-A+}). Cell lysates were evaluated by immunoblotting.

D, E A549 cells were infected for 4 h with WT or *P. aeruginosa* mutants ($\Delta pscD$, ΔSTY , ΔS , and ΔTY). Cell lysates were evaluated by immunoblotting.

Source data are available online for this figure.

by *P. aeruginosa* containing ExoS with only ADPRT activity (S^{G-A+}), (Fig 5C). These experiments suggested that only ADPRT activity of single cytotoxin ExoS was required for cellular autophagy inhibition.

ExoS ADP-ribosyltransferase activity inhibited mTOR signaling pathway

Because mTOR is a major inhibitor of cellular autophagy (Kim *et al*, 2011), we initially thought that ExoS inhibitory effect on autophagy might be mediated by stimulation of mTOR activity.

We evaluated mTOR activity by monitoring the phosphorylation levels of its downstream targets S6 and 4EBP1. Unexpectedly, cells infected with ExoS-expressing *P. aeruginosa* (WT or ΔTY) exhibited reduced mTOR activity reflected by decreased P-S6 and P-4EBP1, compared to cells infected with ExoS-deficient *P. aeruginosa* ($\Delta pscD$, ΔS or ΔSTY) (Fig 5D and E). Similar results were found in primary NHBE cells infected with various *P. aeruginosa* mutants (Fig EV3C). *P. aeruginosa* containing either ExoT (ΔSY) or ExoY (ΔST), as a single T3SS toxin, did not affect mTOR activity (Fig EV3A). We then wanted to determine if the ADPRT activity of ExoS was responsible for mTOR inhibition. We found that mTOR activity was reduced in cells infected with *P. aeruginosa* (S^{G-A+}) but not in cells infected with *P. aeruginosa* (S^{G+A-}) or *P. aeruginosa* (S^{G-A-}) (Fig 5F). Taken together, these data suggested that ExoS ADPRT activity was required and sufficient to inhibit mTOR signaling pathway.

Pseudomonas aeruginosa ExoS ADP-ribosyltransferase activity inhibited mTOR through the inhibition of Ras signaling pathway

Previous studies have shown that *P. aeruginosa* ExoS ADP-ribosylates RAS and inhibits its activity by promoting the hydrolysis of Ras-bound GTP to GDP (Barbieri & Sun, 2004). Because Ras signaling has been implicated in mTOR activation (Mihaylova & Shaw, 2011), we sought to determine if mTOR inhibition by ExoS was caused by Ras ADP ribosylation. We transfected A549 cells with a constitutively active form of Ras (G12V) (Ganesan *et al*, 1998) and found an increase in p-ERK and p-S6 (Fig 6A), suggesting that Ras (G12V) was functional in increasing the activity of Ras pathway in these cells. We then infected these cells with *P. aeruginosa* (ΔTY and ΔSTY). In A549 cells, transfected with empty vector only, infection of *P. aeruginosa* (ΔTY) resulted in inhibition of mTOR activity (reduced p-S6) and autophagy (reduced LC3II) (Fig 6A). Interestingly, In A549 cells transfected with constitutively active Ras (G12V), the reduction of phospho-S6 but not of LC3II was partially rescued (Fig 6A). These data suggested that ADP ribosylation of Ras contributed to the ExoS-induced inhibition of mTOR activity but not to inhibition of autophagy. We then reasoned that Ras-G12V only partially rescued mTOR activity because Ras-G12V, though constitutively active, was still subjected to ADP ribosylation by ExoS on R41 residue, previously shown to be a target for ADP ribosylation (Ganesan *et al*, 1999a). Therefore, we mutated R41 to K in Ras-G12V to prevent its ADP ribosylation (Fig EV5A). Similar to Ras-G12V, exogenous expression of Ras-G12V&R41K caused phosphorylation

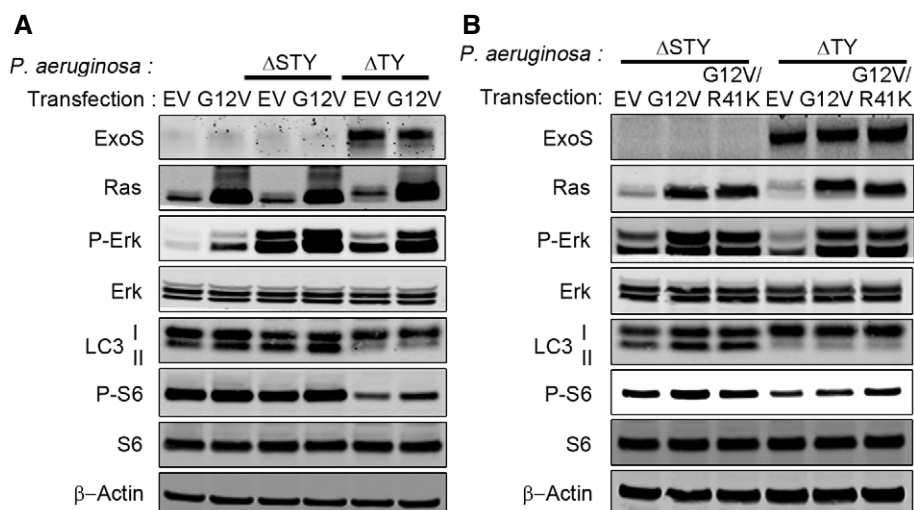


Figure 6. ExoS ADP-ribosyltransferase activity inhibited mTOR through the inhibition of Ras signaling pathway.

A A549 cells were transfected with empty vector (VE) and vector contains Ras-G12V for 24 h, followed by a 4-h infection with *P. aeruginosa* Δ STY or Δ TY. Cell lysates were evaluated by immunoblotting.

B A549 cells were transfected, for 24 h, with empty vector (VE) and vectors contain Ras-G12V or Ras-G12V&R41K followed by a 4-h infection with *P. aeruginosa* Δ STY or Δ TY. Cell lysates were evaluated by immunoblotting.

Source data are available online for this figure.

of ERK and mTOR activation (Fig EV5B). Importantly, in Ras-G12V&R41K expressing cells, *P. aeruginosa* Δ TY infection could still cause significant autophagy inhibition but does not affect TOR activity as no change was found on p-ERK and p-S6 (Fig 6B). These data showed that ExoS's inhibitory effect on mTOR activity was mediated by ExoS-mediated ADP ribosylation of Ras. They further suggested that the ExoS inhibitory effect on autophagy is independent of the activity of either Ras or mTOR.

***Pseudomonas aeruginosa* ExoS ADP-ribosyltransferase activity inhibited autophagic Vps34 lipid kinase activity**

Our data above suggested that ExoS inhibited autophagy initiation rather than autophagic flux and that effect was mTOR-independent. To elucidate the underlying mechanism for autophagy inhibition by ExoS, we evaluated the effect of ExoS on the early initiation events in autophagosome formation. Autophagy initiation depends on the formation of phosphatidylinositol 3-phosphate (PI3P)-enriched omega-somes, which act as platforms to recruit autophagic proteins (Itakura & Mizushima, 2010; Kim *et al.*, 2015). Autophagic pool of PI3P specifically binds to proteins containing FYVE fingers domain such as double FYVE-containing protein 1 (DFCP1); thus, fluorescent DFCP1 has been used as an indicator for PI3P's localization (Itakura & Mizushima, 2010; Kim *et al.*, 2015). We transfected mCherry-DFCP1 into A549 cells, prior to infection with various *P. aeruginosa* mutants. mCherry-DFCP1 puncta were significantly reduced in cells infected with ExoS-containing *P. aeruginosa* (WT and Δ TY), compared to cells infected with ExoS-deficient *P. aeruginosa* (Δ S and Δ STY) (Fig 7A and B). Furthermore, *P. aeruginosa* containing ADPRT-competent ExoS (WT or S^{G-A+}), but not *P. aeruginosa* containing ADPRT-deficient ExoS (S^{G-A-} or S^{G-A-}), inhibited mCherry-DFCP1 puncta's formation (Fig 7A and B). These data suggested that ExoS affected autophagy

PI3P production by the ADPRT activity. Class III phosphatidylinositol 3-kinase Vps34 is the major kinase to produce PI3P (Itakura & Mizushima, 2010; Kim *et al.*, 2015). Vps34 binding with Atg14L to form the Vps34-Beclin1-Atg14L complex, which is implicated in the initiation of autophagosome formation (Kim *et al.*, 2013). We hypothesized that *P. aeruginosa* ExoS inhibited autophagy initiation by inhibiting the activity of Vps34 in the autophagy Atg14L-Vps34 complex. To test this hypothesis, we transfected A549 cells with Flag-tagged Atg14L prior to infecting the cells with various *P. aeruginosa* mutants. The Atg14L-Vps34 complex was immunoprecipitated from cell lysates (Fig 8A). We then determined the kinase activity of Vps34 from the immunoprecipitated Atg14L-Vps34 complex using in vitro lipid kinase assay. Atg14L-Vps34 complex immunoprecipitated from cells infected with ExoS-containing *P. aeruginosa* (WT and Δ TY) had reduced activity, measured by produced PI3P, compared to the immunoprecipitated complex from cells infected with ExoS-deficient bacteria (Δ S and Δ STY) (Fig 8B). These data suggested that ExoS inhibition of Atg14L-associated Vps34 activity as an underlying mechanism for reduced autophagy in *P. aeruginosa*-infected cells. In vitro kinase assay was also performed on Atg14L-Vps34 complex derived from cells infected with *P. aeruginosa* containing various ExoS mutants (S^{G-A-} , S^{G-A+} , S^{G-A+}). Importantly, only the complex derived from cells infected with *P. aeruginosa* with ADPRT-active ExoS (S^{G-A+}) exhibited reduced activity (Fig 8C and D). Taken together, these data suggested that *P. aeruginosa* inhibited host autophagy by a mechanism that involved inhibition of autophagic Vps34 activity by the ADPRT domain of ExoS.

Discussion

The treatment of *P. aeruginosa*, one of the most common bacterial pathogens isolated from hospitalized patients, is often challenging

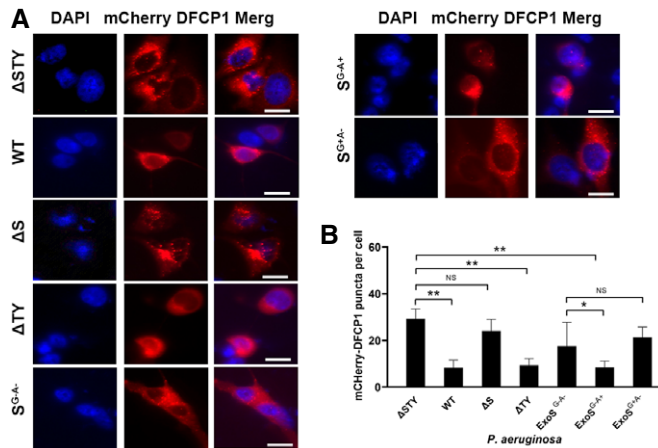


Figure 7. ADP-ribosyltransferase activity of ExoS was required for its effect on omegasome formation.

A A549 cells were transfected, for 48 h, with a mCherry-DFCP1 plasmid and then infected, for 4 h, with *P. aeruginosa* (WT, Δ STY, Δ S, Δ TY, S^{G-A-} , S^{G-A+} , or S^{G-A+}) and the mCherry puncta number per cell was analyzed by fluorescence microscopy. Representative immunofluorescence images were shown, and scale bars represent 10 μ m.

B Quantitative analysis of mCherry-DFCP1 puncta by visually count more than 100 cells for each sample. Each bar represents mean value of from three independent experiments and error bars represent standard deviation. The significance of differences between assays was determined using ANOVA with Dunnett multiple-comparison posttest, NS: not significant; * $P \leq 0.05$; ** $P \leq 0.01$.

Source data are available online for this figure.

due to the high number of multi-drug resistant *P. aeruginosa* strains (Williams *et al.*, 2010). New strategies are required to reduce the morbidity and mortality associated with antibiotic-resistant *P. aeruginosa* infections. Interactions between *P. aeruginosa* and epithelial cells are critical in the development of most infections. These interactions depend largely on the spectrum of effectors secreted by the bacterial T3SS (Vance *et al.*, 2005). The secretion systems in *P. aeruginosa* represent particularly appealing targets because they are essential for bacterial virulence, have conserved components, and depend on specific host factors for their toxicity.

The ability of *P. aeruginosa* to invade and replicate inside airway epithelial cells has been shown in several studies (Chi *et al.*, 1991; Goldberg & Pier, 2000; Kazmierczak *et al.*, 2004; Angus *et al.*, 2010). Further, the requirement of *P. aeruginosa* T3SS for the survival of intracellular *P. aeruginosa* has also been suggested (Angus *et al.*, 2010). However, the mechanisms by which *P. aeruginosa* T3SS promoted intracellular bacterial survival have not been fully elucidated. The formation of membranes blebs in epithelial cells by *P. aeruginosa* has been suggested as an intracellular survival strategy used by the bacteria (Angus *et al.*, 2010). The fact that WT *P. aeruginosa* can survive in the cytoplasm of epithelial cells, whereas *P. aeruginosa* T3SS mutants cannot, suggests that inhibition of the host defense pathway by *P. aeruginosa* T3SS may account for *P. aeruginosa* intracellular survival.

Autophagy is a critical intracellular pathway for the elimination of bacteria (Klionsky & Emr, 2000; Rao & Eissa, 2020). *K. pneumoniae* and *P. aeruginosa* are both gram-negative bacteria and are both typical opportunistic pathogens that cause pulmonary infection

(Wang *et al.*, 2019). Lung epithelial cells can actively degrade invading *K. pneumoniae*, and autophagy is critical for such innate host defense (Cortes *et al.*, 2002; Ye *et al.*, 2014). Our study revealed that *P. aeruginosa*, but not *K. pneumoniae*, were able to resist autophagy-mediated elimination. This observation suggested that *P. aeruginosa* has adopted a protective strategy to counter cellular autophagy-mediated elimination. That T3SS-deficient *P. aeruginosa* could be eliminated by autophagy indicated that *P. aeruginosa* utilizes T3SS to resist autophagy-mediated degradation.

Our study identified a new virulence mechanism of *P. aeruginosa* mediated by T3SS. Engulfment of ExoS-deficient *P. aeruginosa* in autophagosomes suggests that the bacteria are eliminated through autolysosomal digestion. The inhibition of autophagy by *P. aeruginosa* ExoS explains why ExoS-containing *P. aeruginosa* survive better within the epithelial cells compared to the ExoS-deficient *P. aeruginosa*. Besides, we have identified ExoS from T3SS as the only toxin that inhibits autophagy. The most remarkable finding of this study is that a single domain of ExoS possessing the ADPRT activity is responsible for the negative regulation of both the mTOR and autophagy pathways in the host cells. The inhibition of mTOR is achieved by ADP ribosylation of Ras, and autophagy is inhibited by reducing the activity of autophagy-associated kinase Vps34 through an ADP ribosylation mechanism. A working model of the roles of *P. aeruginosa* ExoS in inhibiting host cells autophagy and mTOR to facilitate intracellular bacterial survival is depicted in Fig EV5C.

Pseudomonas aeruginosa could inject up to four cytotoxins through the T3SS apparatus. The wild-type strain of *P. aeruginosa* used in this study contains three cytotoxins ExoS, ExoT, and ExoY (Stover *et al.*, 2000). Based on our results, only ExoS had an inhibitory effect on mTOR and autophagy. Although ExoT is highly homologous to ExoS and also contains the ADPRT domain, it did not have similar effects either on mTOR or autophagy. This differential effect is likely due to ExoS's special molecular structure which leads to more promiscuous substrate specificity (Barbieri & Sun, 2004; Sun *et al.*, 2004).

ExoS is a bifunctional protein that contains GAP and ADPRT activities, and it is one of the most well-studied effector proteins (Ganesan *et al.*, 1998; Miao *et al.*, 2008). The ADPRT domain of ExoS has been implicated in several adverse effects in mammalian cells including cell death and cytoskeletal disruption (Hauser, 2009). It has also been linked to bacterial survival and dissemination in mouse models (Rangel *et al.*, 2015). In our study, we have noticed the adverse effects caused by ExoS as described before, namely ExoS-expressing *P. aeruginosa* caused increased cell death in vitro, enhanced bacterial dissemination, and significantly higher level of mortality in vivo compared with the ExoS-deficient mutant (Fig 4). These findings are consistent with the notion that the cytotoxin ExoS contribute to *P. aeruginosa* virulence (Rangel *et al.*, 2015). It also points out the importance of autophagy in airway epithelial cells for the clearance of *P. aeruginosa*. The in vivo results showing that ExoS-deficient *P. aeruginosa* were eliminated more efficiently in normal mice than in autophagy-deficient mice indicates that autophagy in airway epithelial cells is an important defense mechanism against pulmonary pathogens including *P. aeruginosa*.

The ADPRT domain of ExoS was also critical for the survival of intracellular *P. aeruginosa* as this domain inhibits vacuolar acidification. This, in turn, would eventually prevent the degradation of

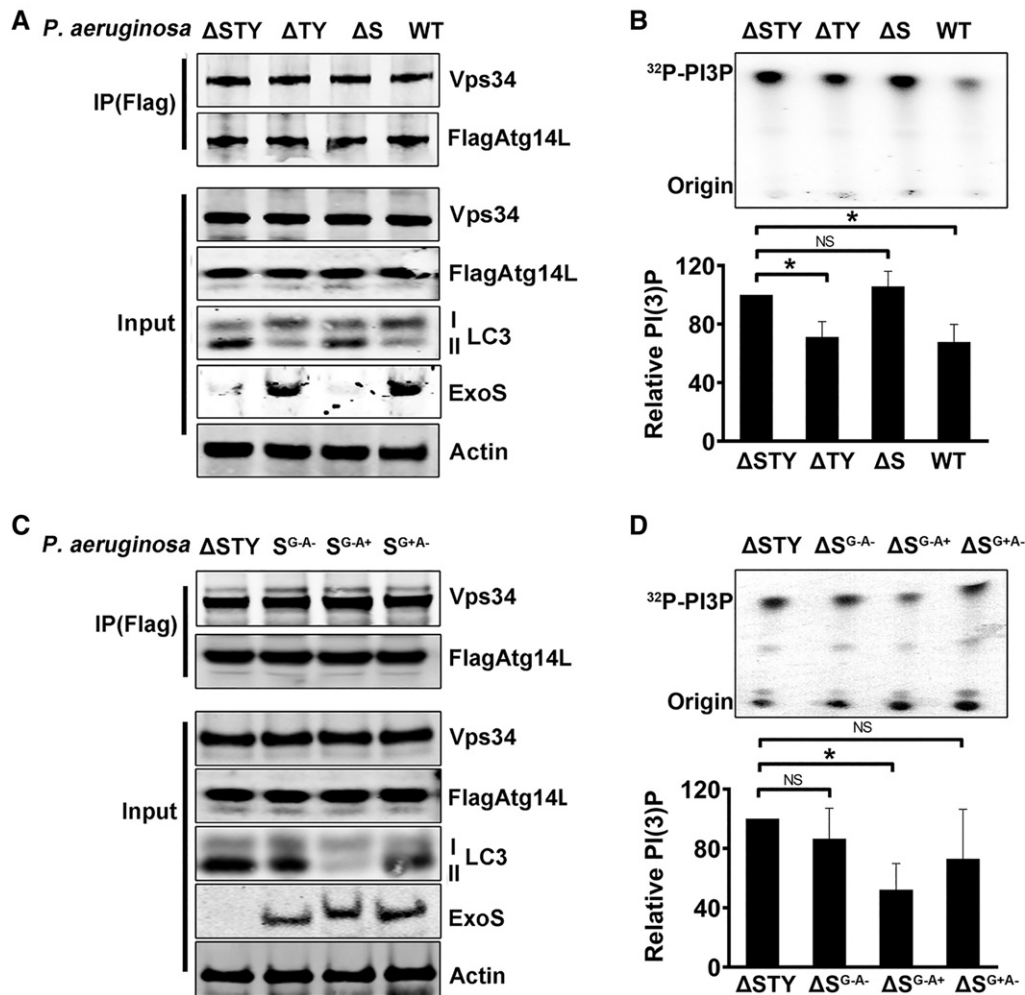


Figure 8. ExoS ADP-ribosyltransferase activity inhibited Vps34 kinase activity.

A, C A549 cells, transfected for 48 h with vector encoding Flag-Atg14L, were infected with *P. aeruginosa* (WT, Δ STY, Δ S, Δ TY, S^{G-A-} , S^{G-A+} , or S^{G+A-}). Flag-Atg14L-Vps34 complex was immunoprecipitated (IP) by Flag-antibody magnetic beads and evaluated by immunoblotting.

B, D The IP complexes were subjected to *in vitro* kinase assay using phosphatidylinositol as substrate. The products radiolabeled PI3P were separated by TLC and detected by autoradiography. Data are mean \pm SD of three independent experiments. The significance of differences between different assays was determined using one-way ANOVA analysis followed Dunn's multiple-comparison posttest, NS: not significant; * $P \leq 0.05$.

Source data are available online for this figure.

the internalized bacterial in the acidified phagolysosome (Angus *et al.*, 2010; Heimer *et al.*, 2013). Our finding that the ADPRT activity of ExoS inhibits autophagy revealed a new mechanism of how this toxin facilitates intracellular bacterial survival. Unlike *Shigella* virulence factor IcsB which facilitate intracellular *Shigella* survival by avoiding autophagy (Ogawa *et al.*, 2005), ExoS from *P. aeruginosa* protects the bacteria by suppressing autophagy. The autophagy pathway involves a cascade of events comprising of multiple proteins and enzymes. In our study, there were no significant changes in protein levels of the key autophagy proteins (Atg7, Atg5, Atg4, Atg3, Beclin1, Atg14L, and LC3) following *P. aeruginosa* infection, suggesting that autophagy was regulated by ExoS at a post-translational level. LC3II is known to be required for specific cargo recognition, and it is one of the first proteins recruited to the site of infection. The Legionella effector cytotoxin RavZ is able to inhibit

autophagy by directly hydrolyzing the conjugated LC3II. Even though ExoS ADP ribosylation domain has a broad substrate specificity, we were not able to demonstrate that LC3I was ADP-ribosylated by ExoS.

The mTOR pathway is a key regulator of autophagy and of cellular growth and metabolism. Some bacteria like *Shigella* and *Salmonella* inhibit mTOR and cause membrane damage. The host cells, in turn, trigger a protective innate immune response, including autophagy activation, to restrain the bacteria (Tattoli *et al.*, 2012). In the case of *P. aeruginosa*, the inactivation of the Ras signaling pathway by ExoS leads to mTOR inhibition, which would otherwise lead to autophagy activation. However, we observed autophagy inhibition with the presence of ExoS which seemed counterintuitive. Our finding that ExoS directly influences the autophagic Atg14L-Vps34 complex kinase activity explains how ExoS caused both mTOR

inhibition and autophagy inhibition at the same time, though by different mechanisms. As mTOR's effect on autophagy is also mediated by ATG14L-Vps34 complex kinase activity (Russell *et al*, 2013), it is likely that the inhibitory effect of ExoS overcomes autophagy induction caused by the inhibition of mTOR.

The autophagic Vps34 complex activity is tightly regulated by ATG14L-Vps34-Beclin1 interaction (Kim *et al*, 2013; Russell *et al*, 2013; Qian *et al*, 2017). Through our study, we did not observe noticeable change in the interaction between Vps34, Beclin1, and ATG14L. Besides, we did not detect the ADP ribosylation of any of the components of the autophagic Vps34 complex. It suggests that autophagic Vps34 complex activity was not directly influenced by ExoS-mediated ADP ribosylation. However, we could not rule out the possibility that ExoS ADPRT activity could indirectly affect Vps34 kinase molecular conformation, which could also result in the reduction of its kinase activity because conformational changes in Vps34 can affect its kinase activity without affecting its interactions with ATG14L or Beclin1 (Qian *et al*, 2017). A greater understanding of how exactly *P. aeruginosa* ExoS ADPRT activity inhibits autophagy could provide insights into novel therapeutic strategies to combat this difficult-to-treat pathogen. Additionally, a therapeutic compound targeting the ExoS ADPRT could be used not only to prevent ExoS-mediated cytotoxic effects but also to benefit *P. aeruginosa* elimination via autophagy.

Materials and Methods

Antibodies and reagents

Antibodies used: rabbit anti-LC3 (Novus); rabbit anti-Atg7 (Santa Cruz, sc-33211); mouse anti-SQSTM1/P62 (Santa Cruz, sc-28359); rabbit anti-phospho-S6 ribosomal protein (Cell Signaling, #2211); mouse anti-S6 ribosomal protein (Cell Signaling, #2317); rabbit anti-Beclin1 (Cell signaling, #3495); rabbit anti-phospho-4EBP1 (Cell Signaling, #9451); rabbit anti-4EBP1 (Cell Signaling, #9644); rabbit anti-phospho-ERK (Cell Signaling, # 4377); rabbit anti-ERK (Cell Signaling, # 9102); rabbit anti-Ras (Cell Signaling, #3965); mouse anti-Actin (Ambion, #AM4302); mouse anti- β -Tubulin IV (Sigma, T7941); rabbit anti-ExoS, ExoT, ExoY were gifts from Dr. Arne Rietsch (Case Western Reserve University, Ohio); rabbit anti-Vps34 (Cell Signaling, #4263); rabbit anti-Atg14L (Cell Signaling, #5504); rabbit anti-*Pseudomonas aeruginosa* (Abcam, ab37057); Rapamycin (Sigma, R0395); Chloroquine, (Sigma, C6628); *m*-Iodobenzylguanidine hemisulfate salt, (Sigma, I9890); Cetrimide Agar, (Sigma, 22470); Gentamycin, (Sigma, G1522-10ML).

Plasmids

Ras-G12V&R41K mutant was generated from a pCDNA3 plasmid containing the Ras G12V sequence (a gift from Dr. Seamus J. Martin). All mutant plasmids were verified by sequencing. pEGFP-ExoS, pEGFP-ExoS^{G⁺A⁻}, pEGFP-ExoS^{G⁻A⁻} obtained from Shouguang Jin's laboratory (University of Florida). Plasmids mCherry-DFCPI (item #86746) were purchased from Addgene. RFP-GFP-LC3 was constructed based on pEGFP-LC3 (Plasmid #21073 Addgene) by in-frame insertion of RFP gene between NheI and AgeI. pcDH GFP-LC3-B was obtained by subclone of GFP-LC3-B into a pcDH-

CMV-mcs-GF1-puro vector (SBI System Biosciences, CD510B-1). Plasmid express Flag-Atg14L was provided by Dr. Xu Qian in Zhimin Lu's laboratory from MD Anderson Cancer Center.

Cell culture

A549 cells were obtained from the American Type Culture Collection (ATCC) and cultured in Ham's F-12K media (Corning) supplemented with 10% fetal bovine serum (FBS), 50 IU/ml penicillin, and 50 μ g/ml streptomycin. Normal human bronchial primary epithelial cells (NHBE) were obtained from Lonza (CC-0225) and maintained in bronchial epithelial cell growth medium with Growth Supplements (Lonza CC-3170). Differentiated epithelial cells were achieved as described previously by plated the cells onto semipermeable membrane inserts (Corning) and cultured at the air/liquid interface (Sha *et al*, 2009). All cells cultures were maintained at 37°C in humidified 5% CO₂ cell culture incubator.

Generation of stable cell line

Atg7-deficient A549 stable cell line A549-(Atg7⁻), was generated using a shRNA against Atg7 (Sigma, Mission shRNA, TRCW000007584). Atg7 shRNA was packed into a lentivirus system (SBI, System Bioscience, CD500) and used to transduce A549 cells. A549 cells stably expressing Atg7 shRNA were maintained in the presence of puromycin (1 μ g/ml). A549 cells stably expressing a non-targeting scrambled shRNA were used as control. A549 cell stably expressing GFP-LC3 was generated using lentiviral vector pcDH GFP-LC3-B and maintained in the presence of puromycin (1 μ g/ml). Other plasmids transfection was performed using Lipofectamine LTX (Life Technologies) according to its manufacturers' protocol.

Bacterial strains and infection

Klebsiella pneumonia (#43816TM) obtained from ATCC. *Pseudomonas aeruginosa* wide type and mutants obtained from Dr Arne Rietsch's laboratory (Cisz *et al*, 2008). Bacterial cultures were grown in Luria-Bertani (LB) broth at 37°C with vigorous shaking. Overnight grown of bacterial were diluted 1:5 and grown for 2 more hours. Bacterial cultures were collected by centrifugation 2,000 \times g for 5 min, washed in phosphate-buffered saline (PBS), centrifuged and normalized to 2 \times 10⁹ colony-forming unit (CFU)/ml. The general infection protocol for cell was as follow: (i) a monolayer of cells was washed three times with PBS, (ii) bacteria were suspended in F12K media supplemented with FBS but with no antibiotics at a multiplicity of infection of 10 bacteria per cell, (iii) cells and bacterial incubated in 5% CO₂ at 37°C for 4 h unless otherwise indicated.

Colony-forming unit assay

A549 cells (1 \times 10⁵ cells per well) were plated in 12-well plate 1 day prior to infection. Cells were inoculated with bacteria at a multiplicity of infection (MOI) of 10 and incubated for 1 or 4 h at 37°C/5% CO₂. Cells were then treated for 1 h with gentamycin 100 μ g/ml to kill extracellular bacteria. Cells were then washed three times with PBS and lysed with 1 ml of 0.1% Triton X-100 in PBS. Lysates

(10 μ l) were plated in LB agar in 10-fold dilutions, and CFU were determined by direct counting after 18 h. In experiments involving rapamycin, cells were treated with rapamycin (0.8 μ g/ml) 18 h prior to infection.

Immunoblot analysis

Cells were washed with PBS and then lysed in Triton X-100 lysis buffer (40 mM Bis-Tris propane, 150 mM NaCl, adjust pH to 7.7, 10% glycerol, 1% Triton X-100) in presence of protease and phosphatase inhibitor cocktail (Thermo Scientific). Equal amount of protein was separated by NuPAGE Bis-Tris-Gel (Novex, life technologies) and transferred onto nitrocellulose membranes. The membranes were incubated with the appropriate antibodies, and the blots were analyzed with Odyssey imaging detection system (LI-COR).

Fluorescence microscopy and flow cytometry

Cells were fixed with 4% paraformaldehyde for 10 min, permeabilized with 0.2% Triton X-100 for 20 min and mounted using the Slow Fade Gold antifade reagent with DAPI (Invitrogen) and visualized with a Zeiss Axiovert 200M microscope. For trachea immunofluorescence staining, 6- μ m mouse trachea frozen sections were fixed in 4% paraformaldehyde for 10 min at room temperature, blocked with 10% normal goat serum (NGS), and then incubated with antibodies. Autophagy analysis was done based on published guideline (Klionsky *et al*, 2008) Fluorescence of GFP-LC3 or mCherry-DFCP1 puncta was counted with at least 10 independent visual fields at 400 \times magnification, and triplicate samples were counted in each experimental condition. To detect the cell viability, 1×10^6 cells were harvested and washed three times with PBS and then resuspend into flow cytometry buffer containing 5 μ l of SYTOXTM Green (Thermo Fisher) or propidium iodide stock solution (Thermo Fisher). With an incubation of 5 min the stained cells were analyzed on LSR Fortessa flow cytometer (BD Biosciences). Data were acquired through FACS Diva (BD Biosciences) and analyzed with FlowJo software (TreeStar).

Transmission electron microscopy

Cells were fixed in 2% formaldehyde +2.5% glutaraldehyde in 0.1 M Millonig's phosphate buffer, pH 7.4 for 2 h at room temperature, postfixed in 1% OsO₄ in 0.1 M Millonig's phosphate buffer for 1 h, dehydrated with increasing concentration of ethanol (70, 95, 100%), and infiltrated with Spurr's Low Viscosity Resin. The sections were cut at 60–70 nm on an RMC MT-6000XL ultra-microtome with a Diatome Ultra45 diamond knife. Cells were stained *en bloc* in saturated uranyl acetate dissolved in 50% ethanol during the dehydration phase of processing and were then visualized with a Hitachi H7500 transmission electron microscope equipped with a Gatan US1000 2 Mp camera and Digital Micrograph software, v1.82.366 to capture images.

Mice

FOXJ1-Cre transgenic mice were purchased from Jackson Laboratory. Atg7^{flox/flox} mice which containing Atg7 gene flanked by LoxP sites were obtained from Dr Masaaki Komatsu's laboratory.

Transgenic mice with Atg7 conditionally knockout in ciliated airway epithelial cell were generated by crossing FOXJ1-Cre mice to Atg7^{flox/flox} mice. Mice were housed within a specific pathogen-free vivarium and used at 4–12 weeks of age. The Baylor College of Medicine's Institutional Animal Care and Use Committee approved all animal studies.

Isolation of tracheal epithelial cells

Tracheas were collected from mice, sliced longitudinally and kept overnight in DMEM/F12 media supplemented with pronase (1.5 mg/ml), DNase I (0.1 mg/ml), penicillin (50 IU) and streptomycin (50 μ g/ml). Next day, protease activity was halted using 10% FBS and the mixture was inverted several times to dislodge cells from tracheas. Tracheas were removed using a cell strainer. Contaminating fibroblasts were removed by adherence to plastic. Epithelial cells in suspension were collected by centrifugation and cultured in bronchial epithelial cell growth media in collagen-coated 6-well plates.

In vivo P. aeruginosa infection

Mice were anesthetized with isoflurane, and 20 μ l of PBS containing a non-lethal dose of *P. aeruginosa* (3×10^7 CFU) was instilled to the airway by inhalation through the nasal opening. After 24 h, different organs were excised and homogenized in PBS solution and homogenized using an OMNI TIP Homogenizing kit (OMNI International, TH-02) under aseptic condition. Lysates were plated in Cetrimide Agar plates in 10-fold dilutions and CFU were determined by direct counting. For mice survival studies, a lethal dose of *P. aeruginosa* (1×10^9 CFU) were injected into mice intranasally and mice mortality were monitored for 10 days.

Immunoprecipitation and Vps34 lipid kinase assay

Flag-tagged ATG14L in the Vps34 complex was immunoprecipitated using a Pierce crosslink Magnetic Co-IP Kit (Thermo Scientific: 88805). Vps34 kinase activity was done, as previously described (Munson & Ganley, 2016). Briefly, phosphatidylinositol (Avanti, 840042) was dissolved in reaction buffer to produce stable 2 mg/ml phosphatidylinositol liposome by passing through Mini extruder set (Avanti, 610000). Immunoprecipitated ATG14L-Vps34 complex was suspended in 60 μ l of reaction buffer containing phosphatidylinositol. The reaction was started by adding 1 μ M ATP and 1 μ Ci 32P- γ -ATP (PerkinElmer, NEG002A) and incubated at ambient temperature for 30 min. The reaction was stopped by adding chloroform: methanol: 12 M HCl (100:200:3.5, *v/v*) and then subjected to phase-split by the addition of 180 μ l chloroform and subsequently 300 μ l 0.1 M HCl. Extracted phospholipid products were separated by thin layer chromatography (TLC) using a coated silica gel and a solvent composed of Methanol/Chloroform/H₂O/14.5 M NH₄OH (47:60:11.2:2, *v/v*). The TLC gels were dried and exposed by autoradiography to visualize the production of isotope labeled PI3P.

Statistics

Statistical analyzed were performed with GraphPad Prism8. All data tested for significance are from at least three independent

experiments. Differences between two groups were compared using Student's *t*-test. Multiple comparison was analyzed using one-way ANOVA analysis following different comparison test as specified in figure legend. *P* value of 0.05 was considered significant.

Data availability

All data of this study are present in the paper or provided as supporting materials. No data deposited in a public database.

Expanded View for this article is available online.

Acknowledgements

We thank current and former members of the Eissa laboratory for useful discussions and technical assistance. We thank Dr. Arne Rietsch for wild-type and mutants of *Pseudomonas aeruginosa*; Drs. Shouguang Jin and Joanne Engel for ExoS plasmids; Dr. Xu Qian and Zhimin Lu for Atg14L plasmid and Dr. Seamus J. Martin for the Ras vectors. This study was supported by funding from the National Heart, Lung and Blood Institute.

Author contributions

Conceptualization, LR, IDLR, and NTE; Performed experiments, LR, IDLR, YX; Methodology and Data analysis, LR, IDLR, YX, YS, AB; Reagents & Resource, MJH, BEG, and NTE; Writing—original draft, LR and IDLR; Writing—review & editing, LR, IDLR, MJH, BEG, and NTE.

Conflict of interest

The authors declare that they have no conflict of interest.

References

- Angus AA, Evans DJ, Barbieri JT, Fleiszig SM (2010) The ADP-ribosylation domain of *Pseudomonas aeruginosa* ExoS is required for membrane bleb niche formation and bacterial survival within epithelial cells. *Infect Immun* 78: 4500–4510
- Barbieri JT, Sun J (2004) *Pseudomonas aeruginosa* ExoS and ExoT. *Rev Physiol Biochem Pharmacol* 152: 79–92
- Chi E, Mehl T, Nunn D, Lory S (1991) Interaction of *Pseudomonas aeruginosa* with A549 pneumocyte cells. *Infect Immun* 59: 822–828
- Cisz M, Lee PC, Rietsch A (2008) ExoS controls the cell contact-mediated switch to effector secretion in *Pseudomonas aeruginosa*. *J Bacteriol* 190: 2726–2738
- Cortes G, Alvarez D, Saus C, Alberti S (2002) Role of lung epithelial cells in defense against *Klebsiella pneumoniae* pneumonia. *Infect Immun* 70: 1075–1080
- Crystal RG, Randell SH, Engelhardt JF, Voynow J, Sunday ME (2008) Airway epithelial cells: current concepts and challenges. *Proc Am Thorac Soc* 5: 772–777
- Diamond G, Legarda D, Ryan LK (2000) The innate immune response of the respiratory epithelium. *Immunol Rev* 173: 27–38
- Ganesan AK, Frank DW, Misra RP, Schmidt G, Barbieri JT (1998) *Pseudomonas aeruginosa* exoenzyme S ADP-ribosylates Ras at multiple sites. *J Biol Chem* 273: 7332–7337
- Ganesan AK, Mende-Mueller L, Selzer J, Barbieri JT (1999a) *Pseudomonas aeruginosa* exoenzyme S, a double ADP-ribosyltransferase, resembles vertebrate mono-ADP-ribosyltransferases. *J Biol Chem* 274: 9503–9508
- Ganesan AK, Vincent TS, Olson JC, Barbieri JT (1999b) *Pseudomonas aeruginosa* exoenzyme S disrupts Ras-mediated signal transduction by inhibiting guanine nucleotide exchange factor-catalyzed nucleotide exchange. *J Biol Chem* 274: 21823–21829
- Goldberg JB, Pier GB (2000) The role of the CFTR in susceptibility to *Pseudomonas aeruginosa* infections in cystic fibrosis. *Trends Microbiol* 8: 514–520
- Hauser AR (2009) The type III secretion system of *Pseudomonas aeruginosa*: infection by injection. *Nat Rev Microbiol* 7: 654–665
- Heimer SR, Evans DJ, Stern ME, Barbieri JT, Yahr T, Fleiszig SM (2013) *Pseudomonas aeruginosa* utilizes the type III secreted toxin ExoS to avoid acidified compartments within epithelial cells. *PLoS One* 8: e73111
- Itakura E, Mizushima N (2010) Characterization of autophagosome formation site by a hierarchical analysis of mammalian Atg proteins. *Autophagy* 6: 764–776
- Jia J, Wang Y, Zhou L, Jin S (2006) Expression of *Pseudomonas aeruginosa* toxin ExoS effectively induces apoptosis in host cells. *Infect Immun* 74: 6557–6570
- Jia K, Thomas C, Akbar M, Sun Q, Adams-Huet B, Gilpin C, Levine B (2009) Autophagy genes protect against *Salmonella typhimurium* infection and mediate insulin signaling-regulated pathogen resistance. *Proc Natl Acad Sci USA* 106: 14564–14569
- Kazmierczak BI, Mostov K, Engel JN (2004) Epithelial cell polarity alters Rho-GTPase responses to *Pseudomonas aeruginosa*. *Mol Biol Cell* 15: 411–419
- Kim J, Kundu M, Viollet B, Guan KL (2011) AMPK and mTOR regulate autophagy through direct phosphorylation of Ulk1. *Nat Cell Biol* 13: 132–141
- Kim J, Kim YC, Fang C, Russell RC, Kim JH, Fan W, Liu R, Zhong Q, Guan KL (2013) Differential regulation of distinct Vps34 complexes by AMPK in nutrient stress and autophagy. *Cell* 152: 290–303
- Kim YM, Jung CH, Seo M, Kim EK, Park JM, Bae SS, Kim DH (2015) mTORC1 phosphorylates UVRAG to negatively regulate autophagosome and endosome maturation. *Mol Cell* 57: 207–218
- Klionsky DJ, Abeliovich H, Agostinis P, Agrawal DK, Aliev G, Askew DS, Baba M, Baehrecke EH, Bahr BA, Ballabio A et al (2008) Guidelines for the use and interpretation of assays for monitoring autophagy in higher eukaryotes. *Autophagy* 4: 151–175
- Klionsky DJ, Emr SD (2000) Autophagy as a regulated pathway of cellular degradation. *Science* 290: 1717–1721
- Levine B, Deretic V (2007) Unveiling the roles of autophagy in innate and adaptive immunity. *Nat Rev Immunol* 7: 767–777
- Li Y, Wang Y, Liu X (2012) The role of airway epithelial cells in response to mycobacteria infection. *Clin Dev Immunol* 2012: 791392
- Loesberg C, van Rooij H, Smets LA (1990) Meta-iodobenzylguanidine (MIBG), a novel high-affinity substrate for cholera toxin that interferes with cellular mono(ADP-ribosylation). *Biochem Biophys Acta* 1037: 92–99
- Miao EA, Ernst RK, Dors M, Mao DP, Aderem A (2008) *Pseudomonas aeruginosa* activates caspase 1 through IpaF. *Proc Natl Acad Sci USA* 105: 2562–2567
- Mihaylova MM, Shaw RJ (2011) The AMPK signalling pathway coordinates cell growth, autophagy and metabolism. *Nat Cell Biol* 13: 1016–1023
- Munson MJ, Ganley IG (2016) Determination of VPS34/PIK3C3 Activity in vitro Utilising 32P-gammaATP. *Bio Protoc* 6: e1904
- Nakagawa I, Amano A, Mizushima N, Yamamoto A, Yamaguchi H, Kamimoto T, Nara A, Funao J, Nakata M, Tsuda K et al (2004) Autophagy defends cells against invading group A *Streptococcus*. *Science* 306: 1037–1040

- Ogawa M, Yoshimori T, Suzuki T, Sagara H, Mizushima N, Sasakawa C (2005) Escape of intracellular Shigella from autophagy. *Science* 307: 727–731
- Qian X, Li X, Cai Q, Zhang C, Yu Q, Jiang Y, Lee JH, Hawke D, Wang Y, Xia Y et al (2017) Phosphoglycerate kinase 1 phosphorylates Beclin1 to induce autophagy. *Mol Cell* 65: 917–931.e6
- Rangel SM, Diaz MH, Knoten CA, Zhang A, Hauser AR (2015) The role of ExoS in dissemination of *Pseudomonas aeruginosa* during pneumonia. *PLoS Pathog* 11: e1004945
- Rao L, Eissa NT (2020) Autophagy in pulmonary innate immunity. *J Innate Immun* 12: 21–30
- Russell RC, Tian Y, Yuan H, Park HW, Chang YY, Kim J, Kim H, Neufeld TP, Dillin A, Guan KL (2013) ULK1 induces autophagy by phosphorylating Beclin-1 and activating VPS34 lipid kinase. *Nat Cell Biol* 15: 741–750
- Scheetz MH, Hoffman M, Bolon MK, Schulert G, Estrellado W, Barabouitis IG, Sriram P, Dinh M, Owens LK, Hauser AR (2009) Morbidity associated with *Pseudomonas aeruginosa* bloodstream infections. *Diagn Microbiol Infect Dis* 64: 311–319
- Sha Y, Pandit L, Zeng S, Eissa NT (2009) A critical role for CHIP in the aggresome pathway. *Mol Cell Biol* 29: 116–128
- Stover CK, Pham XQ, Erwin AL, Mizoguchi SD, Warrenner P, Hickey MJ, Brinkman FS, Hufnagle WO, Kowalik DJ, Lagrou M et al (2000) Complete genome sequence of *Pseudomonas aeruginosa* PAO1, an opportunistic pathogen. *Nature* 406: 959–964
- Sun J, Maresso A, Kim J-J, Barbieri J (2004) How bacterial ADP-ribosylating toxins recognize substrates. *Nat Struct Mol Biol* 11: 868–876
- Sun Y, Karmakar M, Taylor PR, Rietsch A, Pearlman E (2012) ExoS and ExoT ADP ribosyltransferase activities mediate *Pseudomonas aeruginosa* keratitis by promoting neutrophil apoptosis and bacterial survival. *J Immunol* 188: 1884–1895
- Tattoli I, Sorbara MT, Vuckovic D, Ling A, Soares F, Carneiro LA, Yang C, Emili A, Philpott DJ, Girardin SE (2012) Amino acid starvation induced by invasive bacterial pathogens triggers an innate host defense program. *Cell Host Microbe* 11: 563–575
- Vance RE, Rietsch A, Mekalanos JJ (2005) Role of the type III secreted exoenzymes S, T, and Y in systemic spread of *Pseudomonas aeruginosa* PAO1 *in vivo*. *Infect Immun* 73: 1706–1713
- Wang K, Chen Y, Zhang P, Lin P, Xie N, Wu M (2019) Protective features of autophagy in pulmonary infection and inflammatory diseases. *Cells* 8: 123
- Williams BJ, Dehnbostel J, Blackwell TS (2010) *Pseudomonas aeruginosa*: host defence in lung diseases. *Respirology* 15: 1037–1056
- Yasmin L, Jansson AL, Panahandeh T, Palmer RH, Francis MS, Hallberg B (2006) Delineation of exoenzyme S residues that mediate the interaction with 14-3-3 and its biological activity. *FEBS J* 273: 638–646
- Ye Y, Li X, Wang W, Ouedraogo KC, Li Y, Gan C, Tan S, Zhou X, Wu M (2014) Atg7 deficiency impairs host defense against *Klebsiella pneumoniae* by impacting bacterial clearance, survival and inflammatory responses in mice. *Am J Physiol Lung Cell Mol Physiol* 307: L355–363
- Yuan K, Huang C, Fox J, Laternus D, Carlson E, Zhang B, Yin Q, Gao H, Wu M (2012) Autophagy plays an essential role in the clearance of *Pseudomonas aeruginosa* by alveolar macrophages. *J Cell Sci* 125: 507–515